Lifetime Assessment for Glass Fiber Reinforced Plastic (GFRP) Gliders

Volker Trappe, Stephan Günzel and Fabian Grasse
Federal Institute for Materials Research and Testing (BAM),
Unter den Eichen 87, 12205 Berlin, Germany
volker.trappe@bam.de

Ocke Meister
Institute of Aircraft Design and Lightweight Structures, Technical University of Braunschweig,
Hermann-Blenk-Straße 35, 38108 Braunschweig, Germany

Abstract

In a research project fatigue, tests on two identical wing sections that are used as representative substitute components were performed to estimate lifetime enhancement of light-weight aircraft such as general aviation gliders. Single-step fatigue tests at limit load on one component were compared with spectrum loading on the other. A characteristic damage behavior was observed. Local buckling due to high shear loading of the sandwich core of the wing shell caused the main damage. Even though an intentionally high load level was chosen, no increase of micro-cracking could be detected. Additionally, no delamination effects in laminates or bondings were observed except the skin-core delamination which caused the buckling effect in the wing shell due to fatigue loading. Finally, the concept of using representative substructures and accompanying specimen tests is an effective approach for in-service loading investigations and could also be applied to research on wind turbine blades.

Introduction

Several gliders and aircraft for general aviation applications were built in the early 60`s using GFRP-technology. These older models have either reached or are close to their lifetime maximum limit of 12,000 flight hours. The research project "Damage State and Strength" - launched by the Federal Aviation Administration (LBA) and founded by the Federal Ministry of Transport, Building and Urban Affairs (BMVBW) with the partners Federal Institute for Materials Research and Testing (BAM), Institute of Aircraft Design and Lightweight Structures (IFL) and several others (see acknowledgement) – deals with the characterization of the damage state of fiber-reinforced plastics (FRP) under real loading conditions[1]. The focus of these investigations was gliders because their certified maximum strain is about 50 % higher than for airliners or wind turbine blades.

Calculated life span or operating time extensions according to component checks, as is the case with metal designs, is at present not certified for FRP-constructions and is the subject of the present work. Therefore, two identically manufactured wing sections that are used as a representative substructure were tested for indications of component fatigue using two similar test rigs and by applying combined bending and torsion loading with respect to the real loading conditions as well as the maximum certified design values (see Fig. 1 and Fig. 2).

The questions addressed are: What kind of characteristic damage occurs for gliders with light weight wing constructions typically made from FRP? Does the simulated in service load ing compared to the load spectrum KoSMOS[2] lead to the same kind of damage behavior as in a single-step fatigue test at limit load? Do the first signs of micro-cracking indicate the beginning of composites degradation as estimated from specimen studies published elsewhere[3]?

Experimental X-ray-refraction and grey scale value analysis

This approach uses the increase of micro-cracks in GFRP as an indication of the start of material degradation as a result of interlaminar fatigue[4] and can be investigated with two different optical methods: X-ray-refraction[5,6] and grey scale value analysis. In the following, these two methods are briefly presented.

X-ray-refraction

X-ray refraction topography[5,6] is caused by the effect of refraction at the interface of materials with different refractive indices, well known from visible light passing through a glass lenses (see Fig. 3). In the case of X-rays, the refraction angle is below half a degree and in opposite direction due to the dispersion function of isolators. In the experimental setup a collimated X-ray beam passed the sample. At a fixed angle the refracted signal was measured and additionally a signal proportional to the material absorption. A characteristic refraction value C was determined, which is proportional to the inner surface area per unit volume. It can be calculated from the

scattering I_R and transmitted intensities I_A and the thickness d of the sample in relation to the zero values:

$$C = ((I_R / I_{R0}) / (I_A / I_{A0}) - 1) / d \qquad (1)$$

The intensity of the refracted beam will increase if the difference of the refractive index rises at the observed interfaces. Therefore, the intensity will be higher for materials with debonded fibres or pores than without. By calibration the absolute as well as the relative inner surfaces area were measured. In most cases, the relative increase was sufficient and used in the further investigations. Scanning the whole area of the sample gave a topographic map of inner surfaces[3]. It is practical to normalize equation 1 to ln (I_A / I_{A0}) resulting in the relative specific surface C/μ, independent from variation of the number of fibre filaments/sample thickness due to non-perfect production[4]. This approach uses Lambert-Beer's law where the absorption is a function of the density-proportional linear absorption coefficient μ and the thickness d of the sample. In the following investigations, only the average value over the whole sample area was regarded. The short wavelength of the X-ray (Mo-radiation – 0.07 nm) enables detection of defects in the range of 100 nm (1/100 of the fibre diameter).

The determination of the inter-fibre fracture of a single layer is employed to estimate the layer-wise strength of a complex laminate. The influence of the adjacent layers was ignored. Apart from partially large deviations between theory and reality the problem remains that for any semi-finished materials with textile reinforcement, no single layer strength can be stated. Thus, the indication of material parameters (inter-fibre-fracture-strength), essential for construction, is not possible and an understanding of failure processes in complex layer composites is impossible. To solve these problems, X-ray refraction was applied during tensile loading[4]. An electro-mechanical loading facility (MINIMAT) was integrated into the X-ray refraction machine and fixed on a manipulator enabling the loaded sample to be scanned and the refraction values measured. The load was applied in steps until failure of the sample. At each load step a refraction scan was performed. 0°/90°-GFRP-laminates made from woven glass fibre fabrics of linen style (285 g/m²) were investigated as a typical semi finished product for light weight aircraft. This laminate is suited for applications with intralaminar transverse loading and micro-cracking due to inter-fibre failure effects are well known[3].

In Fig. 4, the results from the experiment on the 0°/90°-GFRP-sample are presented. The stress and the relative increase of the refraction values due to micro-cracking caused by inter-fibre fracture processes were plotted versus the strain. Two similar tests were performed. The strain was measured with strain gauges on the samples. Only the transverse cracks in the 90°-layers are oriented parallel to the collimation slits and generate the refraction effect. The increase of micro-cracking in a saturated state is in good correlation with the

change from non-linear to linear mechanical behaviour[4]. In the 0°/90°-laminate a simple inter-fibre transverse loading occurred and the statistically appearance of micro-cracking could be approximated with a Weibull-distribution (see Fig. 5):

$$F = 1 - (e ^ { (-\sigma / \beta) ^ \alpha}) \quad \text{and } f = dF / ds \qquad (2)$$

$$\alpha, \beta \text{ parameter}$$

The function is scaled with the experimentally derived $\Delta C100\%/\mu$ of the saturated state multiplicatively. All parameters are listed in Table 1.

Grey scale value analysis

In GFRP-specimens with adequate quality under conditions of high static or cyclic loading, opaque discoloration of the composite occurs[3]. This discoloration is based on the same refraction effect as the X-ray-refraction. However, the refraction effect occurs if the crack opening is at least about 1000 wavelength of the used light. In the grey scale value analysis, the wavelength of the light is 5,000 to 10,000 times larger than the X-ray-radiation (visible spectrum 300...700 nm) and, hence, the crack opening have to be larger to deploy the refraction effect. Furthermore, using visible light in the grey scale analysis, the absorption due to the refraction effect is larger than by X-rays. Hence, with the crack opening the absorbed intensity of visible light increases while the inner surface proportional X-ray-refraction keeps in a saturated state. However, an increasing grey scale parameter indicates micro-cracking qualitatively correct.

On account of the increase of the micro-crack density the measured light intensity changes. The grey scale value parameter G is defined as

$$G = 1 - (I / I_0) \qquad (3)$$

I_0 designates the intensity of an illuminated background screen and I the intensity through the sample. By normalization of each grey scale measurement to the background value, the parameter is independent of variations of the environment light. The grey scale value analysis was performed with a customary digital camera, which allowed a manual exposure setting and an external control. The grey scale values of the region of interest (ROI) can be determined by self-developed software based on MATLAB.

The grey scale value analysis was applied to GFRP samples accompanying mechanically loading with a conventional servo-hydraulic tensile testing machine (INSTRON 8800) which enables the measurement of the increase of micro-cracking online static and cyclic loading. The same 0°/90°-GFRP-specimens of small size (cross-section 1 x 4 mm) were tensile tested in this testing machine while simultaneously measuring grey scale values similar to the X-ray-refraction online-experiment. The stress/strain curves are compared in

Fig. 5. As estimated, the grey scale value analysis indicates the increase of micro-cracking at increased stress levels. As expected, due to crack closure, the grey scale value decreased when the sample failed. However, remaining micro-cracks were still visible (see Fig. 5). In contrast to the X-ray-refraction method, grey scale value analysis can be easily adapted to a conventional tensile testing machine and, therefore, is an interesting approach. Consequently, grey scale value analysis was adapted to component test for indicating intralaminar fatigue effects due to micro-cracking.

Buckling of sandwich structures with foam core

The classical wing buckling design of gliders is based on the isotropic metal buckling theory. For sandwiches with a flexible core it is important to consider shear deformation as well as bending deformation. The ratio of both deformations is influenced by the core index, a ratio of bending stiffness and core shear stiffness. The buckling load decreases with an increasing core index. While the core shear buckling dominates for values above 0.5, values above 1 cause pure shear buckling (see Fig. 6). The stabilizing effect of boundary conditions (like fixed edges) or geometric conditions (like shell structures) decreases with increasing core index. The critical buckling load is underestimated by a classical buckling design because of the low shear stiffness of foam cores.

In addition to global buckling for sandwich structures, local buckling (wrinkling) can be critical. Two modes for wrinkling are possible: a symmetric hourglass mode and an asymmetric snake mode. With an increasing core thickness, the buckling of sandwiches made of orthotropic face layers and isotropic cores changes from global bending buckling to global core shear buckling and directly to snake mode wrinkling. Depending on layer and load directions, wrinkling waves may result in another direction. Vonach[7] describes a solution for the wrinkling problem of sandwiches.

Component and specimen tests

For the component tests, two identically designed and manufactured wing sections were built at Alexander Schleicher GmbH & Co (see Fig. 7). They possessed defined inspection points in the web of the spar at positions of high and low loadings. At these points the foam core in the sandwich was taken out to enable a good visualization of micro-cracks (see Fig. 8). By using a CCD camera system for the endoscope inspection inside the component, every 500 load cycles (LC) in the single step fatigue test at BAM or 6,000 simulated flight hours at IFL, the designated inspection points were investigated. The basic hypothesis of this approach is that the chosen substructure reflects characteristic fatigue indications. However, this GFRP component test is only representative for aircraft of this specific design principle.

Using finite element analysis, the region of the maximum loading resulting from wing design could be located. Additionally, the estimated strain distribution over the length of the spar

was measured and verified with Fibre-Bragg-Grating-Sensors (FBG) positioned as a FBG-array of 8 sensors each 200 mm bonded on the top of each spar-cap, in-between spar and wing-shell (see Fig. 9).

At the BAM, the wing section was loaded in a single-step fatigue test at limit load with a maximum strain of 8 ‰ to shorten the testing period. The maximum loading frequency was f = 0.0833 Hz. The first visible signs of damage occurred after only 180 LC. A buckling of the outer laminate layer was determined easily by visual inspection (see Fig. 10) and was caused by fatigue of the foam core in the sandwich shell due to high shear loading. The wing shell was repaired and the load level reduced by 20 % to a maximum strain of 6.4 ‰ with respect to real loading conditions. However, after 120 LC at this load-level the same damage behavior was identified.

At the IFL the wing section was loaded with the load spectrum KoSMOS-2[2]. This load sequence contains 556,660 LC of various amplitudes representing 6,000 flight hours. After 36,000 simulated flight hours with the maximum strain level of 6.4 ‰, identical damage occurred as shown in Fig. 11. Even with this similar damage, both wing-sections bore the limit load in tension and torsion in a static test. However, the torsional loading was taken away and tests on BAM and IFL wing sections were continued at the maximum strain level of 6.4 ‰ - at IFL up to 42,000 simulated flight hours and at BAM up to 20,000 LC. Hence, the wing shell as a weak point was identified (see Fig. 12) and the spar structure had to be investigated further. To continue the experiments and to keep the bending loading until high load cycles, the torsion loading was eliminated to avoid expected catastrophic failure. Now the interest of intralaminar fatigue in the web took centre stage to assure and investigate the fatigue strength of the spar structure.

The specimen tests were proceeded with +/- 45°- and 0°/90°-GFRP-laminate made from the same semi-finished products as the web of the test-component. The +/- 45°-specimens were investigated in a strain-controlled fatigue experiment at 4 ‰, 5 ‰ and 6 ‰ (the 0°/90°-laminates force controlled see below). The loading frequency of f = 0.0833 Hz and the load ratio of R = -0.56 up to 20,000 LC was similar to the BAM-component test and the load ration of the KoSMOS spectrum loading. The specimen dimension for the fatigue experiment was 210 mm x 32 mm and 2 mm thickness. The specimen tests were performed in order to determinate the level at which the increase of micro-cracks could be detected by grey scale analysis (see Fig. 13).

For the 4 ‰-specimen, an increase of the micro-cracks was not recognizable with the naked eye and also there was no increase of the measured grey scale value. At strain-levels of 5 ‰ and 6 ‰, the specimens showed definite micro-cracking which resulted in a systematic increase of the grey scale value.

The 0°/90°-specimens were investigated in force-controlled mode up to 200,000 LC with stress-levels of 66, 82 and 100 MPa and with a load ratio R = -1. It was detected an increase of grey scale value for all stress-levels. Even at 66 MPa,

which means a strain of 3 ‰, there was a small measurable increase of the grey scale value, however, at higher numbers of load cycles, up to 200,000. The 100 MPa specimens were broken at approximately 60,000 LC and had the highest increase in grey scale value. The damage was indicated by the sudden increase of the grey scale value parameter approximately 5,000 LC before rupture.

Discussion

Due to the short wavelength of X-rays, the inter-fibre failure in a 0°/90°-GFRP-laminate can be detected far below the transverse strength limit. Compared with a grey scale value analysis, it could be shown that the detection of micro-cracking with light in the visible range is not possible until larger loads are applied. However, visual inspection is common and provides a good means to bridge the gap between a safe-life certification and a damage tolerance concept that would enable operating time extensions for light-weight aircraft made from GFRP.

All investigations on GFRP specimens under cyclic loading showed an increase of micro-cracking long before significant indication of delamination within the laminate occurred. The micro-cracking could easily be determined qualitatively using grey scale value analysis.

Due to the load reduction of 20 % at a strain level of 6.4 ‰, no increase of micro-cracks at the inspection-points at the two identical wing sections could be identified up to the 20,000 LC loading limit and 42,000 simulated flight hours. The strain-level at the inspection points in the web is approximately 4 ‰ and the shear deformation about 3 ‰. Hence, compared to the specimen investigations, the fact that no micro-cracking is observed in the components is in good agreement with these results. Finally, the intralaminar fatigue does not seem to be critical and the increase of micro-cracks could not be used as indication for the amount of in-service loading.

The sandwich-wing shell was much more sensitive to fatigue than the GFRP-laminates. Also, the bondings showed no defects. However, using a representative substructure is an efficient way to perform affordable fatigue investigations for light-weight aircraft and could be applied to wind turbine blades. The damage caused by buckling of the wing shell due to fatigue of the foam core appears to be identical for the single-step fatigue test and for the simulated in-service loading. The classical wing design underestimates the critical buckling load. Therefore, reduced buckling factors with consideration of the low core shear stiffness should be applied. This kind of defect seems to be a reliable indication for a high in-service loading. Finally, research on damage tolerance concepts for FRP-primary structures is important especially in regard to estimating life spans for aging aircraft and should be continued.

Conclusion

Two identical wing sections as a representative substructure for light-weight aircraft made from GFRP were tested in single-step fatigue tests at limit load at BAM and with spectrum loading as performed in the in-service fatigue test at IFL. No increase of micro-cracks as a first indication of the degradation of the laminate could be determined for both components. Additionally, no delaminations in the laminates or in bondings were observed. Micro-cracks are caused by the applied load level and can be identified online from X-ray-refraction investigations during tensile loading. However, with conventional grey scale value analysis in the visible range of light, these micro-cracks could not be reliably detected. Using a representative substructure for fatigue investigations efficiently shows that the typical failure behavior for light-weight aircraft was caused by buckling of the wing shell due to fatigue of the foam core in the sandwich. Additionally identical damage was observed in single-step fatigue tests and under spectrum loading.

Acknowledgements

References

[1]Trappe, V. et al: "Zustand und Festigkeit – Charakterisierung des Schädigungszustandes von FVW unter Betriebsbeanspruchung", Endbericht des vom BMVBW geförderten Forschungsvorhabens "Anwendbarkeit analytischer und experimenteller Lebensdauernachweise", Kennzeichen 50.0298/2002, 2007.

[2]Kossira, H., Reinke, W.: "KoSMOS – Ein Lastkollektiv für Leichtflugzeuge", DGLR-Jahrestagung, Hamburg, DGLR-Jahrbuch I, Bonn, 1989.

[3]Trappe, V., Harbich, K.-W.: "Intralaminar fatigue behaviour of carbon fibre reinforced plastics", International Journal of Fatigue 28 (2006), p. 1187ff.

[4]Trappe, V., Ivers, H.: "Determination of Inter-Fibre-Failure in Complex Reinforced Composites", Proceedings of the 16th European Conference of Fracture, Alexandropolis, Greece, 3 – 7 July 2006, Springer ISBN1-4020-4971-4, p. 775 ff.

[5]Hentschel, M. P. et al: "Röntgenkleinwinkelbrechung an Metalldrähten, Glasfäden und hartelastischem Polypropylen", Acta Cryst., A 43 (1987), p. 506.

[6]Hentschel, M. P., Harbich, K.-W., Lange, A.: "Nondestructive evaluation of single fibre debonding in composites by X-ray-refraction", NDT&E International, Vol. 27,5 (1994), p. 275.

[7]Vonach, W. K.: "A General Solution to the Wrinkling Problem of Sandwiches", Fortschritt–Berichte VDI, Nr. 268 (2001)

Table 1

Parameters of the Weibull approximation of data in Figure 5

Laminate	$\Delta C/\mu$ (100%)	Weibull Parameter α	Weibull Parameter β
0° / 90°-GFRP	0,42	2,5	140,0

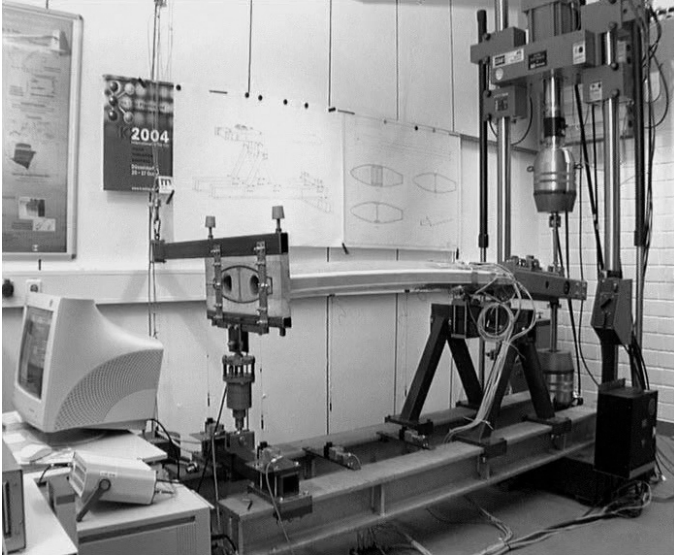**Figure 1** Test rig with wing section at BAM
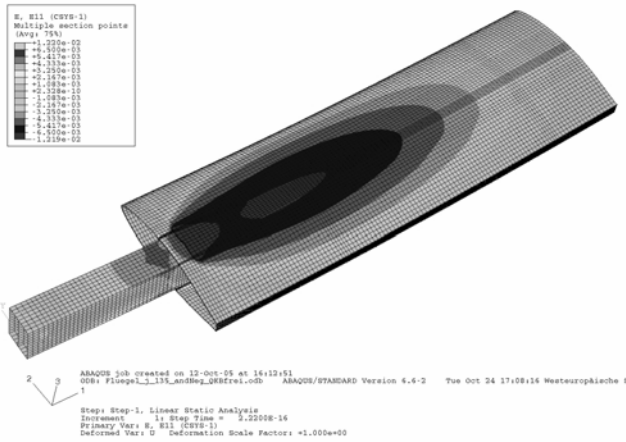
Figure 2 Wing section with defined region of representative max. loading
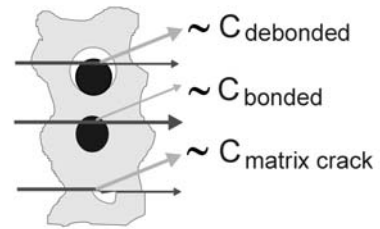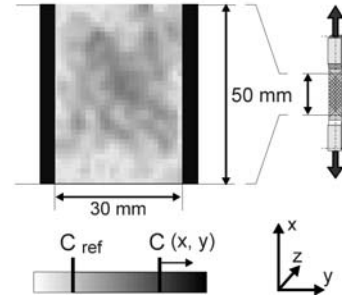
Figure 3 X-ray-refection
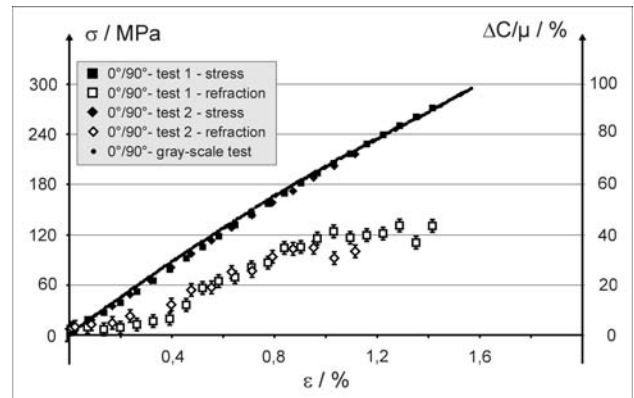
Figure 4 Comparison of stress/strain curves and X-ray-refraction
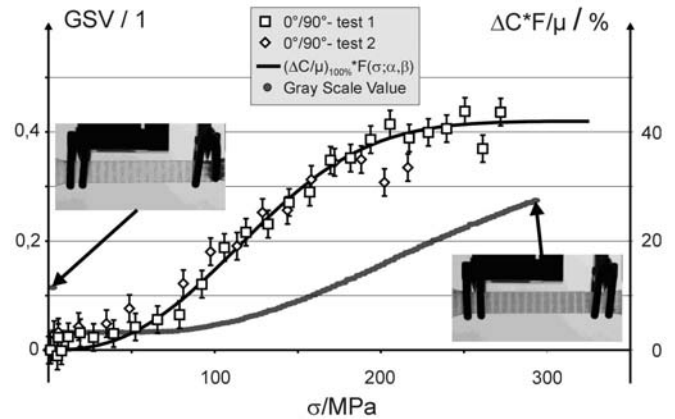
Figure 5 Comparison of X-ray-refraction and grey scale value
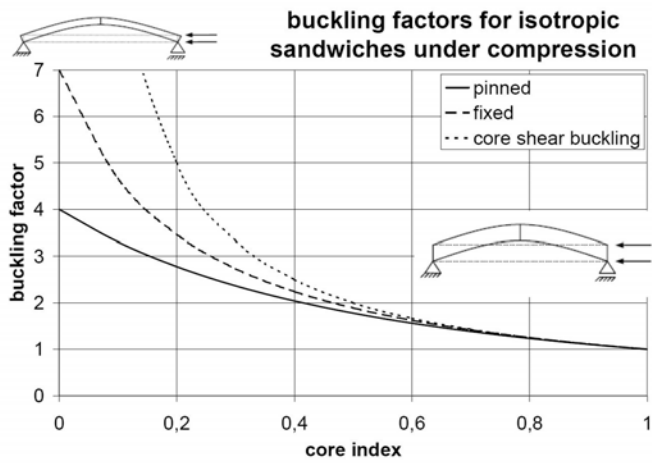
Figure 6 Buckling factors for isotropic sandwiches under compression
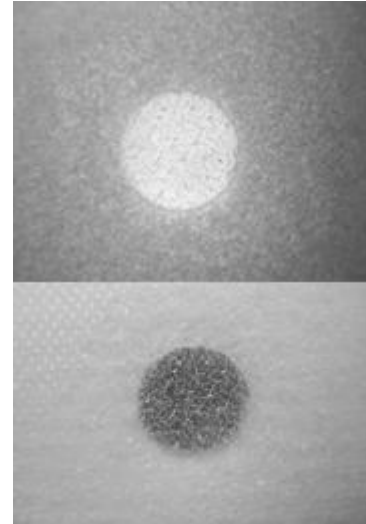
Figure 8 Inspection points of web of the wing spar (backlight and ahead light)

Figure 7 Manufacture of a wing section
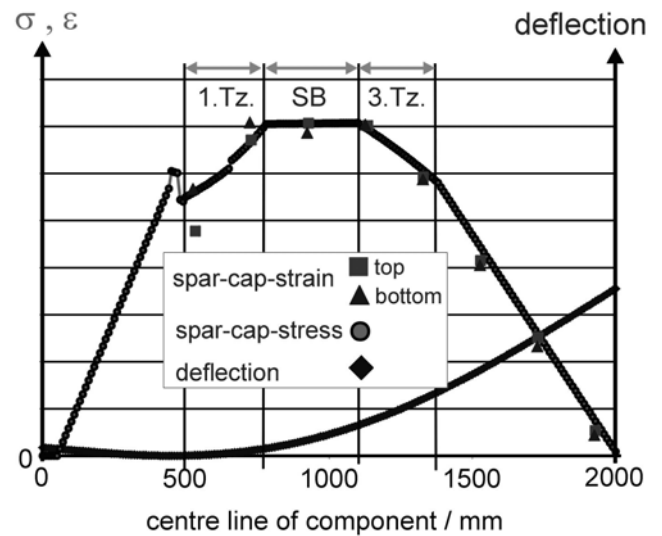
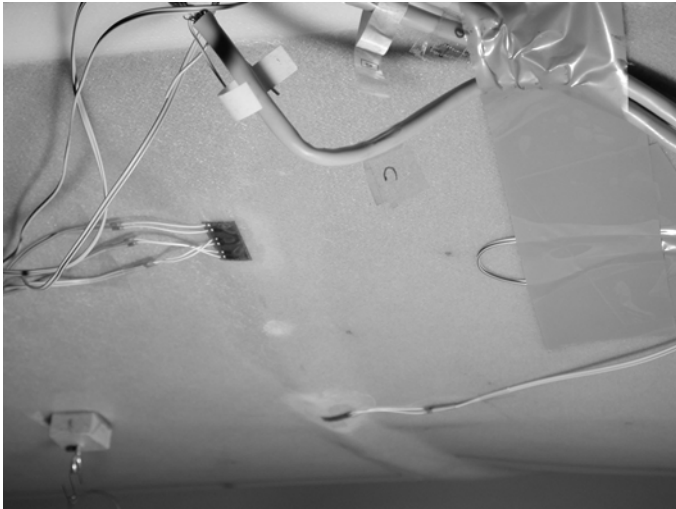**Figure 9** Spar cap stress and deflection (calculated), spar cap strain (measured with FBG´s)

Figure 10 Damage of wing shell at BAM after 180 LC at limit load with a maximum strain of 8 ‰
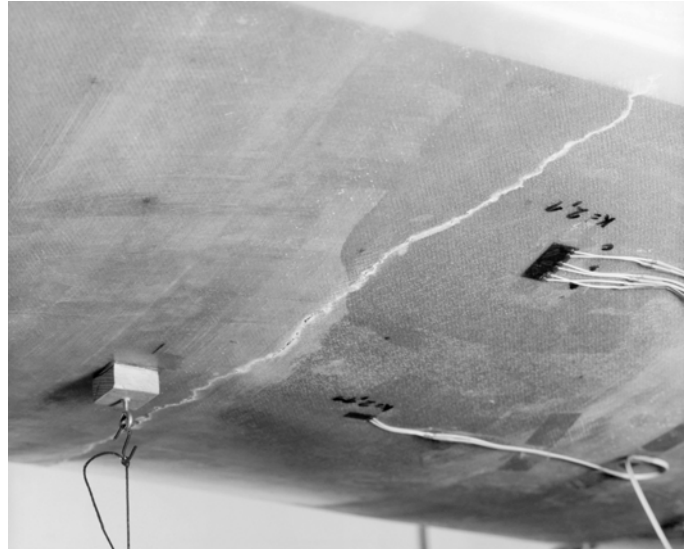

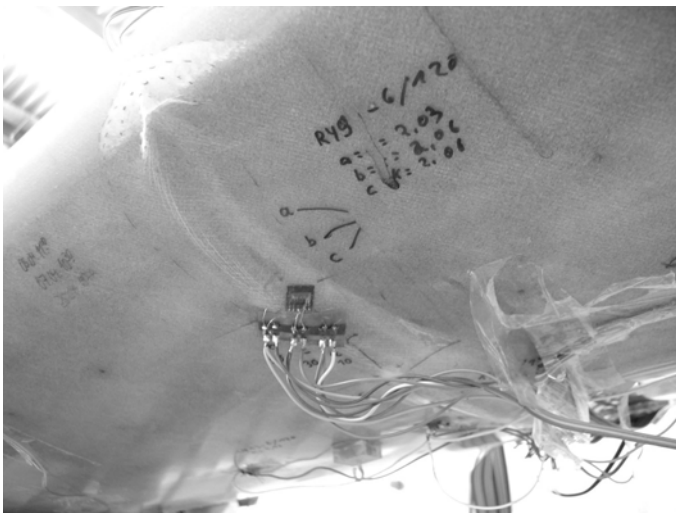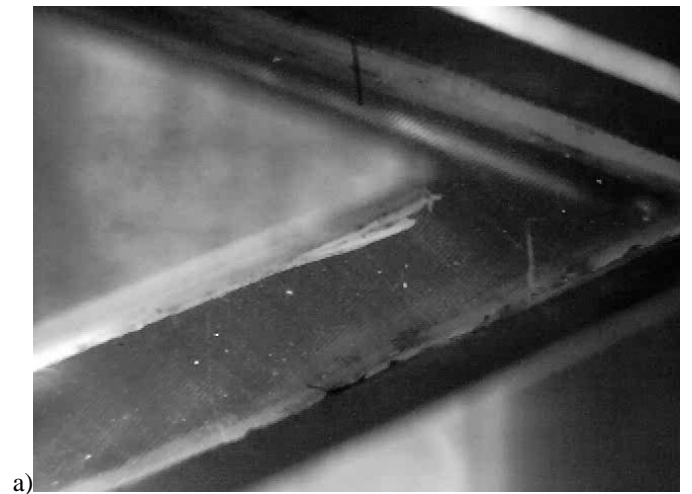**Figure 11** Damage of wing shell at IFL after 36,000 simulated flight hours with the maximum strain level of 6.4 ‰

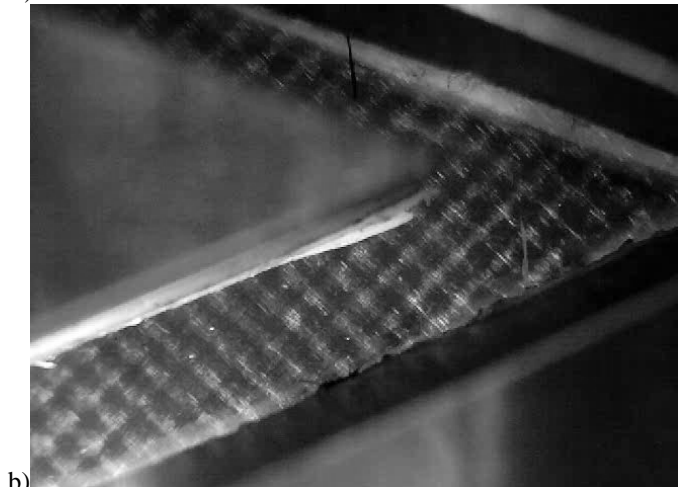**Figure 12** Final damage of wing shell at BAM at reduced load with a maximum strain of 6.4 ‰

a)

b)

Figure 13 GFRP specimen before (a) and after (b) fatigue test with visible micro-cracks